J Membrane Biol (2016) 249:349–361
DOI 10.1007/s00232-016-9873-6

Morphological Effects and Antioxidant Capacity of *Solanum crispum* (Natre) In Vitro Assayed on Human Erythrocytes

Mario Suwalsky[1] · Patricia Ramírez[2] · Marcia Avello[2] · Fernando Villena[3] · María José Gallardo[4] · Andrés Barriga[5] · Marcela Manrique-Moreno[6]

Received: 3 December 2015 / Accepted: 8 January 2016 / Published online: 25 January 2016

Abstract In order to gain insight into the molecular mechanism of the antioxidant properties of *Solanum crispum*, aqueous extracts of its leaves were assayed on human erythrocytes and molecular models of its membrane. Phenolics and alkaloids were detected by HPLC–MS. Scanning electron and defocusing microscopy showed that *S. crispum* changed erythrocytes from the normal shape to echinocytes. These results imply that molecules present in the aqueous extracts were located in the outer monolayer of the erythrocyte membrane. Dimyristoylphosphatidylcholine (DMPC) and dimyristoylphosphatidylethanolamine (DMPE) were chosen as representative of phospholipid classes located in the outer and inner monolayers of the erythrocyte membrane, respectively. X-ray diffraction showed that *S. crispum* preferentially interacted with DMPC bilayers. Experiments regarding its antioxidant properties showed that *S. crispum* neutralized the oxidative capacity of HClO on DMPE bilayers; defocusing microscopy and hemolysis assays demonstrated the protective effect of *S. crispum* against the oxidant effects of HClO on human erythrocytes.

Keywords *Solanum crispum* · Antioxidant activity · Polyphenols · Erythrocyte membrane · Lipid bilayer

Abbreviations

RBC	Red blood cell suspension
SEM	Scanning electron microscopy
DMPC	Dimyristoylphosphatidylcholine
DMPE	Dimyristoylphosphatidylcholine
SEM	Scanning electron microscopy
DM	Defocusing microscopy
Solanum crispum	*S. crispum*
GAE	Gallic acid equivalents
HClO	Hypochlorous acid

Introduction

Solanum crispum Ruíz et Pavón (*S. crispum*), commonly called Natre or Natri, is a plant native to Chile belonging to the *Solanaceae* family. It grows naturally in degraded lands and hillsides, usually between Valparaiso and Chiloe. It is a branchy shrub with dense foliage that reaches three meters high. Its leaves are very dark and bright green, characterized by a strong and intense bitterness. The blue-purple flowers have a very long flowering, while the fruit is a berry of strong bright red color. It is a plant that currently not only enjoys great importance in folk medicine for its antipyretic and anti-hemorrhagic properties, but also has utility against headaches caused by excessive sun exposure. The used parts are the leaves and bark-stripped stems as

✉ Mario Suwalsky
msuwalsk@udec.cl

1 Faculty of Chemical Sciences, University of Concepción, Concepción, Chile

2 Faculty of Pharmacy, University of Concepción, Concepción, Chile

3 Faculty of Biological Sciences, University of Concepción, Concepción, Chile

4 Center for Optics and Photonics, University of Concepción, Concepción, Chile

5 Faculty of Chemical and Pharmaceutical Sciences, University of Chile, Santiago, Chile

6 Faculty of Exact and Natural Sciences, University of Antioquia, Medellín, Colombia

infusion (Muñoz et al. 2004; Schrickel and Bittner 2001; Montes and Wilkomirsky 1991). Chemical studies indicate the presence of coumarins as free scopoletin and its glycosylated form, the steroid β-sitosterol and its glucoside 3-*O*-β-D-glucoside, and the glycoalkaloids solasonine, solasosidine and solanine (Muñoz et al. 2004; Montes and Wilkomirsky 1991). Biological studies support its medicinal benefits as extracts of branches and leaves of the plant have shown antipyretic and anti-inflammatory effects, having been identified scopoletin and the β-sitosterolglucoside in the active fractions (Muñoz et al. 2004). It is known that scopoletin in vitro inhibits prostaglandin synthetase, mechanism that explains its antipyretic effect (Gupta et al. 2011; Ling and Jones 1995). It has also been attributed to scopoletin and its glucoside β-sitosterol for the antimicrobial, hypotensive and smooth muscle relaxant properties (Ling and Jones 1995; Gupta et al. 2011). Moreover, it has been observed that solasodine and the glycoalkaloid solanine exert in arthritis an anti-inflammatory effect similar to cortisol (Manrique-Moreno et al. 2014). Furthermore, studies have been conducted in order to modify the structure of the steroidal alkaloids of this plant to obtain sex hormones and corticosuprarenals (Delporte et al. 1998; Ling and Jones 1995; Shi et al. 2013). The ability of *S. crispum* to act against pathophysiological processes such as inflammation and fever may be related to the fact that oxidative processes are responsible for triggering these symptoms, and it is possible that *S. crispum* is a rich source of active compounds against oxidative stress. Complex mixtures such as plant extracts are formed by compounds of different chemical nature which act together to achieve the same therapeutic effect, which would not be the same if administered separately as single substances.

Aiming to better understand the molecular mechanisms of the antioxidant capacity of *S. crispum*, aqueous extracts of leaves were assayed on human erythrocytes and molecular models of its membrane. Human erythrocytes were chosen because of their only one membrane, and no internal organelles which constitute an ideal cell system for studying interactions of chemical compounds with cell membranes (Chen and Huestis 1997). On the other hand, although less specialized than many other cell membranes, they carry on enough functions in common with them such as active and passive transport, and the production of ionic and electric gradients to be considered representative of the plasma membrane in general. The molecular models of the erythrocyte membrane consisted in bilayers of dimyristoylphosphatidylcholine (DMPC) and dimyristoylphosphatidylethanolamine (DMPE), representative of phospholipid classes located in the outer and inner monolayers of the human erythrocyte membrane, respectively (Boon and Smith 2002; Devaux and Zachowsky 1994). The capacity of *S. crispum* to interact with the bilayer structures of DMPC and DMPE was evaluated by X-ray diffraction; intact human erythrocytes were observed by scanning electron microscopy (SEM) and defocusing microscopy (DM). DM is a previously established light microscopy technique (Agero et al. 2004; Mesquita et al. 2006) based on the visualization and analysis of contrast images of transparent objects like biological organisms seen out of focus. This technique has proven to be very powerful with a large number of applications, such as the morphological characterization of red blood cells (RBCs) (Agero et al. 2004; Etcheverry et al. 2012). These systems and techniques have been used in our laboratories to determine the interaction with and the membrane-perturbing effects of other chemical compounds present in native plant extracts (Suwalsky et al. 2006a, b, 2008, 2009, 2015). The antioxidant properties of *S. crispum* were evaluated in the molecular models of the erythrocyte membrane and human erythrocytes in vitro exposed to the oxidative stress induced by hypochlorous acid. HClO is a powerful natural oxidant that damages bacteria, endothelial cells, tumor cells, and erythrocytes (Tatsumi and Fliss 1994; Zavodnik et al. 2001; Hawkins and Davies 1998; Carr et al. 1997; Suwalsky et al. 2006a, b).

Materials and Methods

Plant Material

The collection of leaves of *S. crispum* was held in September 2012, at the University of Concepcion campus, coordinates 36°49′39″ South, 73°2′20″ West. The plant was identified by the taxonomist Dr. Roberto Rodriguez, Department of Botany of the University of Concepción; a voucher was deposited in the Herbarium under catalog number CONC 176480. The leaves were dried in the shade at room temperature; after drying, they were ground in a blade mill; the homogenized ground plant material was stored in a container with a suitable cover in a cool and dry place until ready to use. Aqueous extracts were obtained by Soxhlet extraction. In order to achieve this, 20 g of ground sample and 250 mL of water were used. The process was conducted for 48 h. The aqueous extract was frozen at −20 °C and then was lyophilized (FDL-10N-50, MRC, Israel). The total return on a dry basis was determined and stored in a cool and dry place until use.

Determination of Total Polyphenols

The total polyphenol content of the aqueous extracts was spectrophotometrically determined (Shimadzu UVmini-1240, Kyoto, Japan) at 765 nm by the Folin–Ciocalteu method (Singleton and Rossi 1965) using Folin–Ciocalteu

reagent (Merck, Germany). Briefly, aliquots of test samples (0.5 mL of 1 % extract) were mixed with 25 mL of distilled water, 2.5 mL Folin–Ciocalteu reagent, 10 mL 20 % Na_2CO_3, and completed to 50 mL with water, shaken, and allowed to react for 30 min. Gallic acid (GA, Sigma-Aldrich, lot 98K0245, MW 170, St. Louis. MO) was used as the standard for a calibration curve and the total polyphenol contents were expressed as gallic acid equivalents (GAE). The determinations were performed in triplicate.

HPLC-Mass Determinations

The *S. crispum* aqueous extract (12.3 mg) was prepared at a concentration of 9.5 mg/mL in methanol–water 1:1 v/v and a volume of 20 μL was analyzed using a LC–ESI–MS/MS system which consisted of the HPLC HP1100 (Agilent Technologies Inc, CA-USA) connected to the mass spectrometer Esquire 4000 Ion Trap LC/MS(n) system (Bruker Daltonik GmbH, Germany). A column Supelcosil LC-18 300 × 4.0 mm, 5 μm, and 120 Å (Sigma-Aldrich Co. LLC, USA) was used for the analysis. On the other hand, at the exit of the column a split divided the eluant for simultaneous UV and mass spectrometry detection. The mobile phase corresponded to formic acid in water (10 % v/v, solvent A) and formic acid in acetonitrile (10 % v/v, solvent B) at a flow rate of 1 mL/min according to the following elution gradient: 0–25 min, 5–15 % B; 25–53 min, 15–27 % B; 53–57 min, 27–5 % B; and 57–60 min, 5 % B. Compounds were detected at 280 nm. Mass spectral data were acquired in positive and negative modes; ionization was performed at 3000 V assisted by nitrogen as nebulising gas at 24 psi and as drying gas at 365 °C and a flow rate of 6 L/min. All scans were performed in the range 20–2200 *m/z*. The trap parameters were set in ion charge control using manufacturer default parameters. Collision-induced dissociation (CID) was performed by collisions with the helium background gas present in the trap and automatically controlled through Smart Frag option.

Scanning Electron Microscopy (SEM) Studies on Human Erythrocytes

Five blood drops (about 100 μL) from a human healthy donor not receiving any pharmacological treatment were obtained by puncture of a finger and received in an Eppendorf tube containing 10 μL of heparin (5000 UI/mL) in 900 μL of saline solution (NaCl 0.9 %, pH 7.4). Red blood cells were then low speed centrifuged (1000 rpm × 10 min) and washed three times in saline solution. The sedimentary washed cells were suspended in 900 μL of saline solution, and fractions of 150 μL of this stock of red blood cells suspension (RBCS) were placed in Eppendorf tubes to prepare (a) the control (RBCS in saline solution) and (b) a range of molar concentrations of aqueous extracts expressed as gallic acid equivalents (GAE); they were centrifuged, supernatant replaced by the solutions under study, and then incubated at 37 °C for 1 h, period in line with the larger effects induced by compounds on red cell shape (Zimmermann and Soumpasis 1985; Malheiros et al. 2000). Incubated samples were centrifuged and the supernatant replaced by 500 μL of 2.5 % glutaraldehyde in distilled water, reaching a final concentration of about 2.4 %. After this fixation, samples were washed three times in distilled water and drops of each one were placed on siliconized glass covered Al stubs, dried at 37 °C, gold coated in a sputter device (Edwards S 150, Sussex, England), and examined in a scanning electron microscope (JEOL JSM-6380LV, Japan).

Defocusing Microscopy (DM) Studies of Human Erythrocytes

The effect of *S. crispum* extracts in red blood cells (RBC) was evaluated by defocusing microscopy (DM), a light microscopy technique based on the visualization and analysis of contrast images seen out of focus. The experiments were done in an inverted optical microscope Nikon Eclipse Ti-U (Nikon, Tokyo, Japan). The objective was mounted on a C-focus system (Mad City Labs, Madison, USA) for a nanometric control of the focal plane position. The visualization was done with a High Resolution CMOS Camera (Thorlabs, New Jersey, USA). To carry out the experiment, three to four drops of blood were obtained from the finger of a healthy donor under no pharmacological treatment. RBC solution was prepared diluting the blood 20 times in a solution of PBS 1× and BSA 1 mg/mL. Stock solution of the *S. Crispum* extract (0.1, 1.0, and 5 mM GAE) was provisioned by following the same preparation of PBS and BSA. In order to carry out the analysis, RBCs diluted solution was placed in a cuvette, and visualized at the optical microscope. After that, a morphologically normal erythrocyte was selected and the concentration of *S. crispum* extract was increased until 2 mM of GAE. To make three-dimensional reconstructions, two images of one erythrocyte were captured in the defocus positions +1 and −1 μm (Etcheverry et al. 2012).

X-ray Diffraction of Phospholipid Bilayers

The capacity of *S. crispum* extract to interact with DMPC and DMPE bilayers was evaluated by means of X-ray diffraction. Synthetic DMPC (lot 140PC-246, MW 677.9) and DMPE (lot 140PE-71, MW 635.9) from Avanti Polar Lipids, AL, USA were used without further purification.

About 2 mg of each phospholipid were introduced into Eppendorf tubes which were then filled with 200 μL of (a) distilled water (control) and (b) aqueous solutions of *S. crispum* extracts in a range of concentrations (0.1 mM up to 0.5 mM in the case of DMPC and 0.5 up to 5 mM for DMPE). The specimens were shaken, incubated for 30 min at 30, and 60 °C with DMPC and DMPE, respectively, and centrifuged at 2500 rpm for 20 min. Samples were then transferred into 1.5 mm diameter special glass capillaries (Glas-Technik & Konstruktion, Berlin, Germany), and X-ray diffracted utilizing Ni-filtered CuKα radiation from a Bruker Kristalloflex 760 (Karlsruhe, Germany) X-ray generator. Specimen-to-film distances were 8 and 14 cm, standardized by sprinkling calcite powder on the capillary surface. The relative reflection intensities were obtained in a MBraun PSD-50 M linear position-sensitive detector system (Garching, Germany); no correction factors were applied. Data analysis was performed by means of Origin 3.0 software (Origin Lab Corp., USA). Experiments were performed at 19 ± 1 °C, which is below the main phase transition temperature of both DMPC and DMPE. Higher temperatures would have induced transitions onto fluid phases making the detection of structural changes harder. Each experiment was repeated in triplicate.

Results

Yield

Total yield of the *S. crispum* aqueous extract was 26.4 %; total polyphenol content is shown in Table 1.

Identification of Phenolic Compounds by HPLC–MS

Table 2 contains the tentative identifications for the 25 chromatographic peaks; the identification was based on: (1) the most intense *m/z* signal of mass spectra obtained for each chromatographic UV peak, (2) correlation between both polarities (however, there were compounds only observed in one ionization mode) and adduct presence, and (3) comparison of experimental fragmentation versus literature and database fragmentation. Based on the identification of the detected compounds, these can be gathered in two main categories: phenolic and alkaloid compounds.

Table 1 Total polyphenol content expressed as gallic acid equivalents (GAE)

Extract	mM GAE	mg GAE/100 g simple
AE	4.05 ± 0.065	6.88 ± 0.115

Results were determined in 1 % extracts

Among detected phenolic compounds, the following could be distinguished: phenolic acids correspondent to caffeoylquinic acid (peaks 3 and 6), dicaffeoylquinic acid (peak 21), and the glucoside of dihydroxybenzoic acid (peak 4); flavan-3-ol as (epi)catechin (peak 16) although it was observed as *m/z* 291 and *m/z* 289 in positive and negative polarity, it was identified through its dimeric form; flavonols such as quercetin (peak 24) including quercetin-*O*-sophorotrioside (peak 11), quercetin-*O*-sophoroside-*O*-glucoside (peak 13), quercetin-*O*-dihexoside (peaks 14 y 15), and quercetin-*O*-hexoside (peaks 19 and 20) or kaempferol in kaempferol-*O*-hexoside (peak 21) and kaempferol-*O*-dihexoside (peak 17); and O-methylated flavonols such as isorhamnetin-*O*-dihexoside (peak 19). Among alkaloid compounds dehydrospirosolane-type and/or solanidane-type alkaloids were detected and observed as *m/z* 414 in peaks 9, 11, 13, 17, and 20 co-eluting with phenolic compounds. Based on the fragmentation of *m/z* 414 in peak 9, it was tentatively identified as a spirosolane-type alkaloid due mainly to its fragmentation in *m/z* 396, *m/z* 274, and *m/z* 253. In the other peaks *m/z* 414 showed the fragments *m/z* 396, *m/z* 253, and *m/z* 271 described at literature as main fragments in dehydrospirosolane-type alkaloid (e.g., tomatidenol) and variable presence in solanidane-type alkaloids (e.g., leptinidine) (Cataldi et al. 2005; Shakya and Navarre 2008). Other chromatographic peaks were not identified. In some cases several peaks were assigned with the same identification due to the presence of isomeric forms.

Scanning Electron Microscopy (SEM) Studies on Human Erythrocytes

SEM examinations of human erythrocytes incubated with *S. crispum* showed that its aqueous extract induced echinocytosis. In that altered condition, red blood cells lost their normal biconcave shape (Fig. 1a) and presented a spiny configuration with blebs in their surfaces (Fig. 1b, c). The extent of these changes was *S. crispum* concentration dependent.

Defocusing Microscopy (DM) Studies of Human Erythrocytes

The erythrocyte morphology through three-dimensional reconstructions was determined using defocusing microscopy. DM observations of human erythrocytes incubated with *S. crispum* showed that the extract induced echinocytosis. Figure 2a shows defocusing microscopy experiments of human red blood cells exposed to different concentration of the aqueous extract of *S. crispum*. This compound induced the transformation of the normal discoid morphology of the erythrocytes to equinocytes

Table 2 Compound identification in aqueous *S. crispum* extract by HPLC–MS

Peak	RT (min)	Precursor (*m/z*)	Fragments MS^2 (*m/z*)						Identification	References
Positive polarity										
1	2.5	209.3	191.5	94.2	176.0			M + H	Kynurenine	Piraud et al. (2003)
2	2.9	–							Not identified	
3	3.6	–								
4	4.1	–								
5	5.5	–							Not identified	
6	6.7	730.9	377.1					2M + Na	Caffeoylquinic acid	
		377.4	359.0	214.7	184.7	331.1	341.1	M + Na	Caffeoylquinic acid	
7	7.1	–							Not identified	
8	7.9	–							Not identified	
9	9.4	481.7	317.1					M + H	Not identified	
		414.1	396.4	273.9	253.0			M + H	Spirosolane-type alkaloid	Cataldi et al. (2005)
										Shakya and Navarre (2008)
10	11.2	739.2	720.8						Not identified	
11	11.5	811.5	509.3	347.2				M + Na	Quercetin-*O*-sophorotrioside	
									Quercetin-*O*-caffeoyl-sophoroside	
		414.6	396.4	253.1	270.8			M + H	Solanidane/dehydrospirosolane-type alkaloid	Cataldi et al. (2005)
										Shakya and Navarre (2008)
12	12.7	–							Not identified	
13	13.6	414.7	396.5	252.9	271.3			M + H	Solanidane/dehydrospirosolane-type alkaloid	Cataldi et al. (2005)
										Shakya and Navarre (2008)
14	14.8	649.7	347.1	487.1				M + Na	Quercetin-*O*-dihexoside	
		627.5	465.0	303.0	447.1			M + H	Quercetin-*O*-dihexoside	
15	15.5	649.6	347.1	329.1	487.1			M + Na	Quercetin-*O*-dihexoside	
		627.0	465.0	303.0	447.0	344.9		M + H	Quercetin-*O*-dihexoside	
16	17.5	291.1						M + H	(Epi)catechin	
17	20.1	633.8	347.1					M + Na	Kaempferol-*O*-dihexoside	
		414.8	396.5	253.1	271.1			M + H	Solanidane/dehydrospirosolane-type alkaloid	Cataldi et al. (2005)
										Shakya and Navarre (2008)
18	20.8	472.9	221.8	310.2	455.3	293.1	233.9	M + H	Not identified	
19	21.8									
20	23.3	950.4	487.1					2M + Na	Quercetin-*O*-hexoside	
		487.5	325.0	184.7				M + Na	Quercetin-*O*-hexoside	
		414.9	396.5	253.2	271.1			M + H	Solanidane/dehydrospirosolane-type alkaloid	Cataldi et al. (2005)
										Shakya and Navarre (2008)

Table 2 continued

Peak	RT (min)	Precursor (*m/z*)	Fragments MS^2 (*m/z*)						Identification	References
21	29.7	471.6	308.9	184.6				M + Na	Kaempferol-*O*-hexoside	
22	36.0	–							Not identified	
23	37.4	739.0	720.8						Not identified	
24	39.1	899.1	880.9	752.8	736.8	410.5	428.5	M + H	Solanidenediol solatriose	Shakya and Navarre (2008)
		865.2	849.7	718.8	702.8	821.7	394.5	M + H	Solanidadienol chacotriose	Shakya and Navarre (2008)
25	40.4	314.3	176.6	144.6				M + H	Not identified	
Negative polarity										
1	2.4	–								
2	2.8	371.1	352.8	190.5	172.4				Not identified	
3	3.6	353.3	190.4	178.5	134.3			M–H	Caffeoylquinic acid	Gouveia and Castilho (2011) Obied et al. (2007) Regueiro et al. (2014)
4	4.0	315.2	152.3	108.3	164.3	224.5		M–H	Dihydroxibenzoicacid-*O*-glucoside	Fang et al. (2002) Shakya and Navarre (2006)
5	5.5	–							Not identified	
6	6.8	707.0	352.8					2M–H	Caffeoylquinic acid	
		375.3	178.4	200.5	134.4	190.5	160.4	M + Na–2H	Caffeoylquinic acid	
		353.2	190.5					M–H	Caffeoylquinic acid	Biesaga and Pyrzynska (2009) Eyles et al. (2007) Oszmiański et al. (2014)
7	7.2	570.9	352.8	216.6				M–H	Not identified	
8	7.9	–							Not identified	
9	9.5	479.4	184.4	346.8				M–H	Not identified	
10	11.3	–							Not identified	
11	11.5	787.5	607.0	299.9	505.0	625.1	354.9	M–H	Quercetin-*O*-sophorotrioside	Lin et al. (2011) Schmidt et al. (2010)
12	12.7	–							Not identified	
13	13.6	787.9	300.8	444.9	667.1	462.9		M–H	Quercetin-*O*-sophoroside-*O*-glucoside	Lin et al. (2011) Schmidt et al. (2010)
14	14.9	625.4	300.8	445.0	505.0	462.9	270.8	M–H	Quercetin-*O*-dihexoside	Alvarez-Suarez et al. (2010) Ferreres et al. (2010) Gouveia and Castilho (2010) Lin et al. (2011) Ye et al. (2005) Zhang et al. (2012)

Table 2 continued

Peak	RT (min)	Precursor (*m*/*z*)	Fragments MS^2 (*m*/*z*)						Identification	References
15	15.7	625.5	299.9	445.0	462.9	504.9	270.8	M–H	Quercetin-*O*-dihexoside	Alvarez-Suarez et al. (2010) Ferreres et al. (2010) Gouveia and Castilho (2010) Lin et al. (2011) Schmidt et al. (2010) Ye et al. (2005) Zhang et al. (2012)
16	17.6	579.2	535.0	244.7	288.4	202.6		2M–H	(Epi)catechin	La Torre et al. (2006)
		288.5						M–H	(Epi)catechin	
17	20.3	609.6	284.8	429.0	446.9	254.7	488.9	M–H	Kaempferol-*O*-dihexoside	Ferreres et al. (2010) Petsalo et al. (2006) Schmidt et al. (2010) Vallverdú-Queralt et al. (2014)
18	21.0	470.6	334.1	291.0	160.3			M–H	Not identified	
19	22.1	639.0	314.8	299.8	458.9			M–H	Isorhamnetin-*O*-dihexoside	Parejo et al. (2004) Schmidt et al. (2010) Truchado et al. (2010)
		463.6	300.8					M–H	Quercetin-*O*-hexoside	Gordon et al. (2011) Gouveia and Castilho (2010)
20	23.5	463.5	300.8					M–H	Quercetin-*O*-hexoside	Gordon et al. (2011) Gouveia and Castilho 2010
21	29.9	515.3	352.8	202.5	447.0			M–H	Dicaffeoylquinic acid	AlGamdi et al. (2011) Gouveia and Castilho (2011) Vallverdú-Queralt et al. (2014) Ye et al. (2005)
		447.5	284.7	326.9	254.8			M–H	Kaempferol-*O*-hexoside	Ferreres et al. (2010) Harbaum et al. (2007) Vallverdú-Queralt et al. (2014) Yang et al. (2011)
22	36.2	–							Not identified	
23	37.7	633.4	457.0	439.1				M–H	Not identified	
24	39.3	301.2	178.4	150.4	256.6	272.6		M–H	Quercetin	Gouveia and Castilho (2010) Gouveia and Castilho (2011) Mullen et al. (2003) Tatsis et al. (2007)
25	40.6	312.3	177.4	296.8	134.3	147.3		M–H	Not identified	

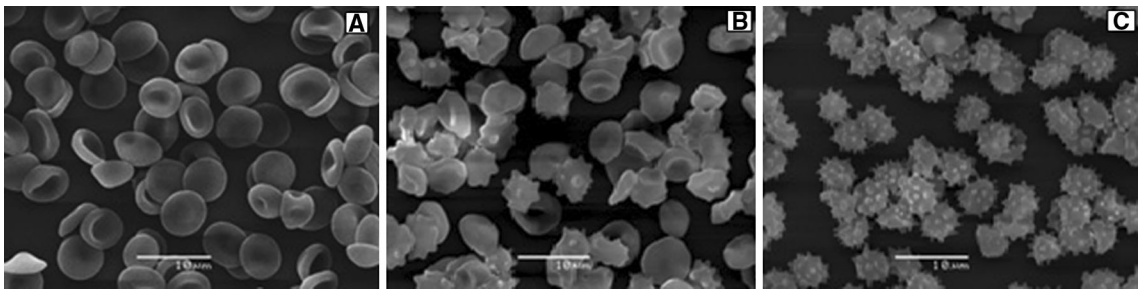

Fig. 1 Effects of *S. crispum* on the morphology of human erythrocytes. Scanning electron microscopy (SEM) images of control (**a**), and incubated with 0.1 mM (**b**) and 0.5 mM (**c**) aqueous extracts of *S. crispum* expressed as gallic acid equivalents (GAE)

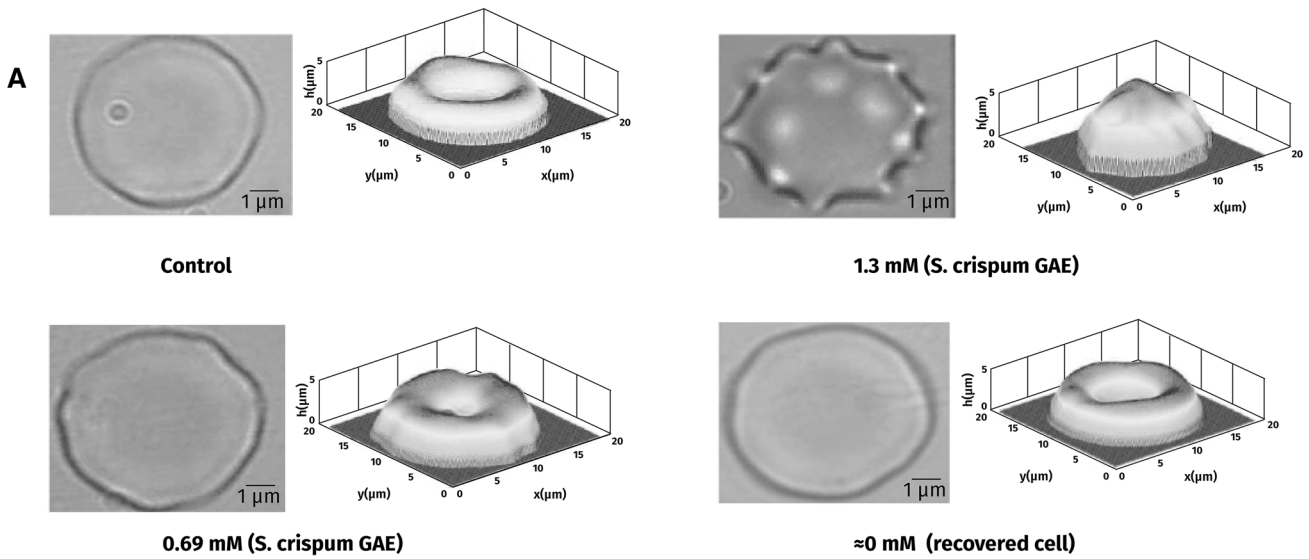

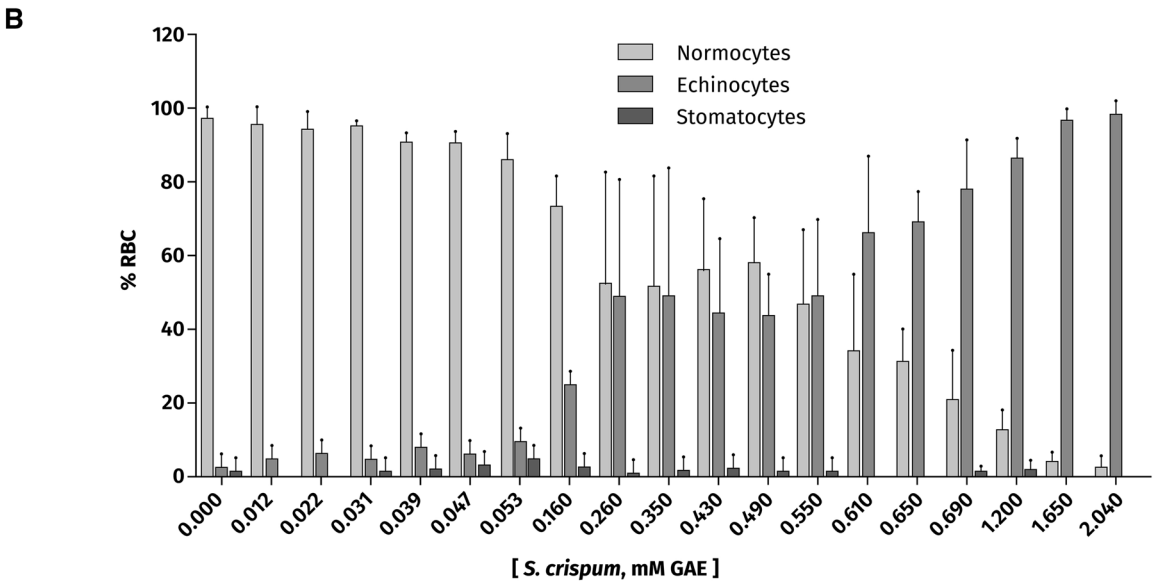

Fig. 2 Effects of *S. crispum* on human erythrocytes. **a** Defocused microscopy (DM) images and three-dimensional reconstructions of untreated erythrocytes (control) and incubated with 0.69 and 1.3 mM of aqueous extracts of *S. crispum*, and the recovered cell. **b** Population distribution of different cell morphologies with different concentrations of aqueous extracts of *S. crispum.* Concentrations are expressed as gallic acid equivalents (GAE)

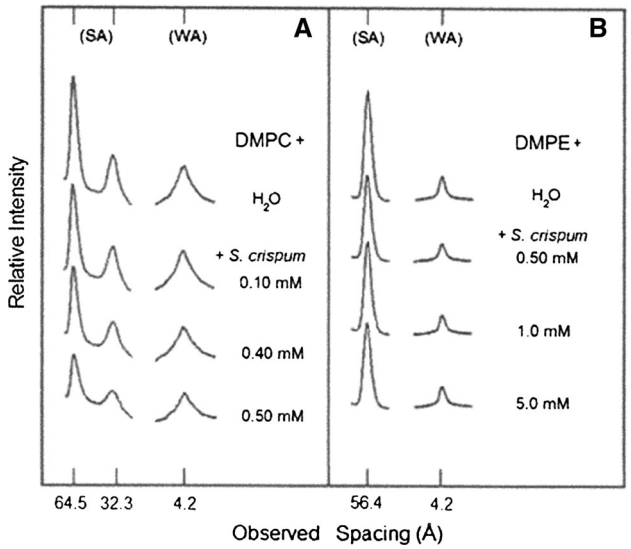

Fig. 3 X-ray diffraction patterns of **a** dimyristoylphosphatidylcholine (DMPC) and **b** dimyristoylphosphatidylethanolamine in water and aqueous extracts of *S. crispum*; (SA) small-angle and (WA) wide-angle reflections. Concentrations are expressed as gallic acid equivalents (GAE)

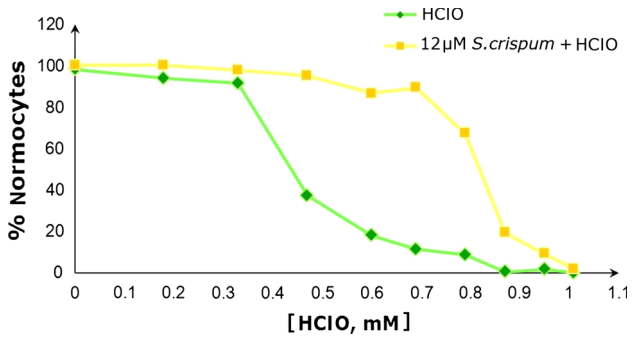

Fig. 4 Antioxidant effects of aqueous extracts of *S. crispum* against human red blood cells exposed to HClO, observed, and counted by optical microscopy. Concentrations are expressed as gallic acid equivalents (GAE) (Color figure online)

reaching a maximum of effect at 2 mM (Fig. 2b). It was observed that this was a reversible process. When the solution was diluted, the cell recovered its original morphology (Fig. 2a).

X-ray Diffraction of Phospholipids Multilayers

Figure 3a exhibits the results obtained by incubating DMPC with water and *S. crispum* aqueous extracts. As expected, water altered the DMPC structure: its bilayer repeat (bilayer width plus the width of the water layer between bilayers) increased from about 55 Å in its dry crystalline form to 64.5 Å when immersed in water and its small-angle

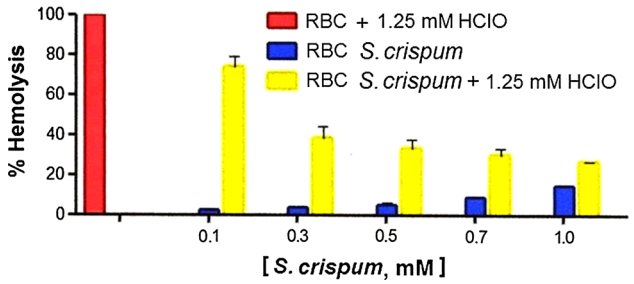

Fig. 5 Percentage of hemolysis of red blood cells (RBC) incubated with 1.25 mM HClO and different concentrations of aqueous extracts of *S. crispum* expressed as gallic acid equivalents (GAE) (Color figure online)

reflections (indicated as SA) were reduced to only the first two orders of the bilayer repeat (Suwalsky 1996). On the other hand, only one strong reflection of 4.2 Å showed up in the wide-angle region (indicated as WA), which corresponds to the average lateral distance between fully extended acyl chains organized with rotational disorder in hexagonal packing. Figure discloses that after exposure to *S. crispum* extracts in the range 0.1 M–0.5 mM GAE, there was gradual weakening of the lipid reflection intensities, particularly those of the small-angle range. From these results, it can be concluded that the extract produced mainly a structural perturbation of the polar region of DMPC bilayers. Results from similar experiments with DMPE are presented in Fig. 3b. The fact that only one strong reflection of 56.4 Å is observed in the small-angle region and the presence of the 4.2 Å in the wide-angle region are indicative of the gel state adopted by DMPE in water after heating and cooling it. Increasing concentrations of the plant extract in the range 0.5–5 mM GAE only induced a very slight gradual decrease of the small-angle reflection intensities. Thus, the molecular content of the extract interacted mostly with DMPC bilayers.

Antioxidant Properties

The antioxidant properties of *S. crispum* were in vitro assayed in human erythrocytes and in phospholipid bilayers exposed to HClO. Experiments were carried out by defocusing microscopy, hemolysis, and X-ray diffraction.

Defocusing Microscopy (DM) Studies of Human Erythrocytes

To observe whether the aqueous extract of *S. crispum* has a protective effect against HClO, RBCs were pre-incubated with low concentrations of the extract (12 μM GAE). Then, the concentration of HClO was increased and the cells were visualized and counted by optical microscopy. In Fig. 4, it can be observed that in RBC pre-incubated with the aqueous extract of *S. crispum* the fraction of stomatocytes decreased compared to the fraction of stomatocytes

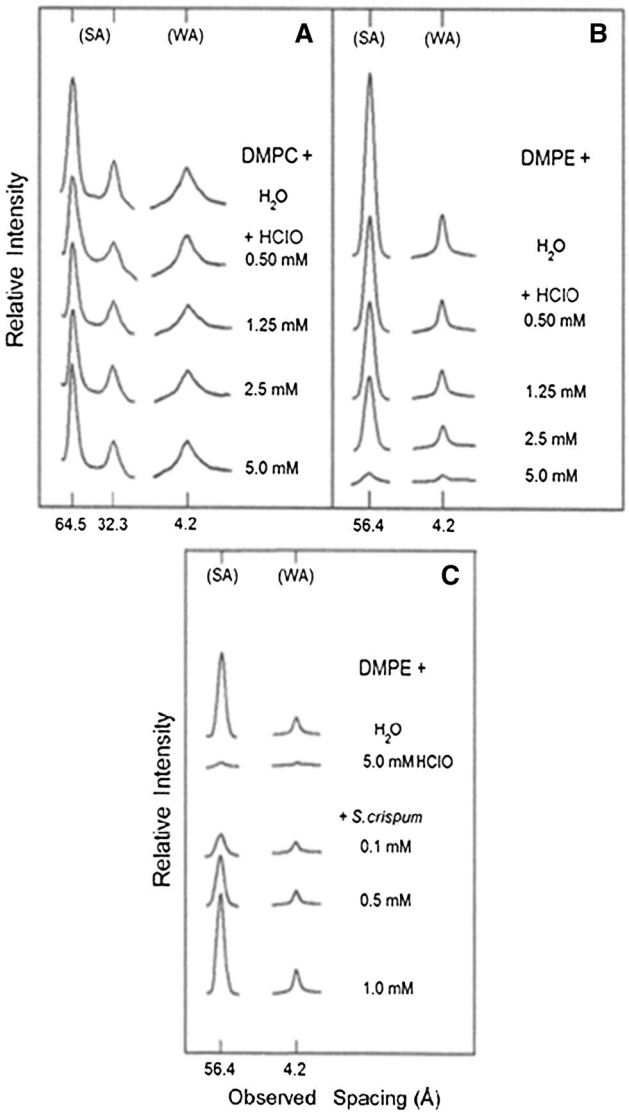

Fig. 6 X-ray diffraction patterns of **a** dimyristoylphosphatidylcholine (DMPC) in water and HClO; **b** dimyristoylphosphatidylethanolamine in water and HClO; **c** dimyristoylphosphatidylethanolamine in water, aqueous extracts of *S. crispum* and HClO; (SA) small-angle and (WA) wide-angle reflections. Concentrations of extract are expressed as gallic acid equivalents (GAE)

incubated only with HClO. Then, the aqueous extract of *S. crispum* has a protective effect in cell morphology change induced by HClO.

Hemolysis Assays

Increasing concentrations of *S. crispum* in the 0.1–1.0 mM GAE range gradually increased the % of hemolysis although to a very low extent (about 15 % with 1 mM GAE *S. crispum*). However, the same range of *S. crispum* concentrations gradually reduced the hemolytic effect of 1.25 mM HClO (100 % hemolysis) which reached a value of 26 % with 1 mM *S. crispum* (Fig. 5).

X-ray Diffraction of Phospholipid Bilayers

Figure 6 shows the different effects of HClO on DMPC and DMPE bilayers. As it can be appreciated in Fig. 6a, HClO in the range of 0.5 up to 5 mM induced no significant structural perturbation to DMPC; however, in the same range of concentration HClO produced an increasing disorder to DMPE bilayers, whose reflection intensities became almost negligible with 5 mM concentration (Fig. 6b). In Fig. 6c, it can be appreciated that increasing concentrations of *S. crispum* in the range 0.1–1.0 mM GAE neutralized the deleterious effects of 5 mM HClO.

Discussion

To the best of our knowledge, there are no specific published reports on the antioxidant property of aqueous extracts of *S. crispum* on cell systems. In the present study, the interaction and antioxidant properties of *S. crispum* was evaluated on human erythrocytes and molecular models of its membrane. The latter consisted in DMPC and DMPE bilayers, classes of lipids preferentially located in the outer and inner monolayers of the human erythrocyte membrane, respectively (Boon and Smith 2002; Devaux and Zachowsky 1994).

SEM and DM observations showed that *S. crispum* induced morphological alterations to red cells from their normal discoid shape to echinocytes. According to the bilayer couple hypothesis (Sheetz and Singer 1974; Lim et al. 2002), the shape changes induced in erythrocytes by foreign molecules are due to differential expansion of the two monolayers of the red cell membrane. Thus, stomatocytes (erythrocytes with cup-like shapes) are formed when the compound inserts into the inner monolayer, whereas spiculated-shaped echinocytes are produced when it locates into the outer moiety. The finding that *S. crispum* induced the formation of echinocytes indicates that molecules were inserted in the outer leaflet of the erythrocyte membrane. This conclusion is supported by X-ray experiments carried out in DMPC and DMPE bilayers. In fact, results showed that *S. crispum* molecules only interacted with DMPC, which is preferentially located in the outer monolayer of the human erythrocyte membrane.

Results by X-ray diffraction on the interaction of *S. crispum* aqueous extract with DMPC bilayers in the gel phase showed that it produced a moderate but significant structural perturbation of the lipid bilayer, this effect being higher in the hydrophilic region of DMPC. On the other hand, no effects were observed in DMPE even at a very high concentration. DMPC and DMPE differ only in their terminal amino groups, these being $^{+}N(CH_3)_3$ in DMPC and $^{+}NH_3$ in DMPE. Moreover, both molecular

conformations are very similar in their dry crystalline phases with the hydrocarbon chains mostly parallel and extended and the polar groups lying perpendicularly to them (Suwalsky 1996). However, DMPE molecules pack tighter than those of DMPC. This effect, due to DMPE smaller polar groups and higher effective charge, stands for a very stable multibilayer system which is not significantly affected by water (Suwalsky and Duk 1987). The strong hydrogen network of DMPE bilayers is certainly a reason for the reduced penetration of water and other compounds into its interfacial head group region. On the other hand, the hydration of DMPC results in water filling the highly polar interbilayer spaces with the resulting width increase (Suwalsky and Duk 1987; Janiak et al. 1976). (For further details regarding PC and PE fully hydrated gel phases, see Katsaras et al. 2000; Mason et al. 2001). This phenomenon might allow the incorporation of molecules present in *S. crispum* aqueous extract into DMPC bilayers and thus inducing the subsequent structural perturbation.

In the present study, the antioxidant capacity of *S. crispum* was assayed on human erythrocytes and DMPC and DMPE bilayers exposed to HClO-induced oxidative stress. HClO is an extremely toxic biological oxidant generated by neutrophils and monocytes, and it is considered one of the most important factors causing tissue injuries in inflammation (Zavodnik et al. 2001). It is directly toxic to bacteria, endothelial cells, tumor cells, and red cells. However, because it readily reacts with a range of biological targets, it has been difficult to identify which reactions are critical for its cytotoxic effects (Vissers et al. 1998). Human erythrocytes are the reliable and easily obtainable model to detect oxidative stress (Battistelli et al. 2005). Their simple internal structure depleted of nucleus and organelles provide an ideal system for this type of study (Chen and Huestis 1997). One major consequence of their exposure to HClO is lysis; although the exact mechanism is not clear, the cell membrane is considered the primary site for reaction. In fact, several studies have demonstrated that HClO treatment of erythrocyte membrane results in inhibition of Na^+, K^+-, and Mg^{2+}-ATPase activities, oxidation of SH^- groups, tryptophan residues, chloramines formation, changes of membrane fluidity and surface area, and membrane morphological transformations, events that precede cell lysis (Zavodnik et al. 2001; Vissers et al. 1998; Vissers and Winterbourn 1995).

As shown in Fig. 6a and b, HClO perturbs to different extents the structures of DMPC and DMPE bilayers, this effect being considerable higher in DMPE. Since both lipids possess the same fully saturated acyl chains of 14 methylene groups, the explanation for the dissimilar HClO effect must be related to the structural differences in their head group regions. In the case of DMPE, the adjacent molecules and bilayers are attached by a network of electrostatic interactions and H-bonds between the amino (H-donating) and phosphate (H-accepting) groups resulting in a very stable flat gel phase. HClO polar molecules (pK 7.53) would disrupt the H-bond net that keep together DMPE molecules by being intercalated between the negatively charged phosphates and positively charged amino groups. On the other hand DMPC, which instead of hydrogen is provided with bulky methyl groups, and the presence of considerable amounts of water between the bilayers make the interbilayer interactions rather small. In this case, HClO molecules would remain mainly in the interbilayer water layers inducing perturbing effects only at considerable high concentrations by disruption of the intermolecular attractions in DMPC bilayer.

DM observations on human erythrocytes showed that HClO induced the formation of stomatocytes. This result is not surprising as the X-ray experiments demonstrated that HClO preferentially interacted with DMPE, class of lipid mostly located in the inner monolayer of the red cell membrane. According to the bilayer couple hypothesis (Sheetz and Singer 1974; Lim et al. 2002), this location of HClO molecules should result in a lateral expansion of the membrane inner monolayer, changing the normal shape of erythrocytes into stomatocytes. DM observations also demonstrated the protective effect of *S. crispum* against the shape perturbing effect of HClO upon human erythrocytes (Fig. 4). Similar results were also obtained in hemolysis assays (Fig. 5). It might be then concluded that the location of *S. crispum* antioxidant molecules into the membrane bilayer might hinder the insertion of HClO and its subsequent damaging effects. This conclusion can also imply that this restriction could apply to the diffusion of free radicals into cell membranes and the consequent decrease of the kinetics of free radical reactions. In conclusion, *S. crispum* would act by blocking access of the oxidants into the lipid bilayer and scavenges them before they can penetrate the cell membrane.

Conclusions

The presence of phenolics in *S. crispum* aqueous extracts of its leaves and their antioxidant properties have been reported for the first time. Results indicated that *S. crispum* leaves possess good antioxidant properties due to the high-phenolic content. Studies performed in human erythrocytes allowed to infer that molecules present in the aqueous extract located into the outer monolayer of the red cell membrane. This conclusion was supported by X-ray studies performed on molecular models of the erythrocyte membrane. It is therefore possible to conclude that the location of *S. crispum* molecules in cell membranes might hinder the diffusion of free radicals into cells.

Acknowledgments This work was supported by FONDECYT (Projects 1130043 and 3140167).

References

Agero U, Mesquita LG, Neves BRA, Gazzinelli RT, Mesquita ON (2004) Defocusing microscopy. Microsc Res Tech. 65:159–165

AlGamdi N, Mullen W, Crozier A (2011) Tea prepared from *Anastatica hirerochunticas* seeds contains a diversity of antioxidant flavonoids, chlorogenic acids and phenolic compounds. Phytochem 72:248–254

Alvarez-Suarez JM, González-Paramás AM, Santos-Buelga C, Battino M (2010) Antioxidant characterization of native monofloral Cuban honeys. J Agr Food Chem 58:9817–9824

Battistelli M, De Sanctis R, De Bellis R, Cucchiarini L, Dacha M, Gobbi P (2005) *Rhodiola rosea* as antioxidant in red blood cells: ultrastructural and hemolytical behavior. Eur J Histochem 49:243–254

Biesaga M, Pyrzynska K (2009) Liquid chromatography/tandem mass spectrometry studies of the phenolic compounds in honey. J Chromatogr A 1216:6620–6626

Boon JM, Smith BD (2002) Chemical control of phospholipid distribution across bilayer membranes. Med Res Rev 22:251–281

Carr AC, Vissers MCM, Domigan NM, Witerbourn CC (1997) Modification of red cell membrane lipids by hypochlorous acid and hemolysis by preformed lipid clorohydrins. Redox Rep 3:263–271

Cataldi TR, Lelario F, Bufo SA (2005) Analysis of tomato glycoalkaloids by liquid chromatography coupled with electrospray ionization tandem mass spectrometry. Rapid Commun Mass Spectrom 19:3103–3110

Chen JY, Huestis WH (1997) Role of membrane lipid distribution in chlorpromazine-induced shape change of human erythrocytes. Biochim Biophys Acta 1323:299–309

Delporte C, Backhouse N, Negrete R, Salinas P, Rivas P, Cassels BK, San Feliciano A (1998) Antipyretic, hypothermic and antiinflammatory activities and metabolites from *Solanum ligustrinum* Lood. Phytother Res 12:118–122

Devaux PF, Zachowsky A (1994) Maintenance and consequences of membrane phospholipids asymmetry. Chem Phys Lipids 73:107–120

Etcheverry S, Gallardo M, Solano P, Suwalsky M, Mesquita ON, Saavedra C (2012) Real-time study of shape and thermal fluctuations in the echinocyte transformation of human erythrocytes using defocusing microscopy. J Biomed Opt 17:106013

Eyles A, Jones W, Riedl K, Cipollini D, Schwartz S, Chan K, Herms DA, Bonello P (2007) Comparative phloem chemistry of Manchurian (*Fraxinus mandshurica*) and two North American ash species (*Fraxinus americana* and *Fraxinus pennsylvanica*). J Chem Ecol 33:1430–1448

Fang N, Yu S, Prior RL (2002) LC/MS/MS characterization of phenolic constituents in dried plums. J Agr Food Chem 50:3579–3585

Ferreres F, Pereira DM, Valentão P, Andrade PB (2010) First report of non-coloured flavonoids in *Echium plantagineum* bee pollen: differentiation of isomers by liquid chromatography/ion trap mass spectrometry. Rapid Commun Mass Spectrom 24:801–806

Gordon A, Jungfer E, da Silva BA, Maia JG, Marx F (2011) Phenolic constituents and antioxidant capacity of four underutilized fruits from the Amazon region. J Agr Food Chem 59:7688–7699

Gouveia SC, Castilho PC (2010) Characterization of phenolic compounds in *Helichrysum melaleucum* by high-performance liquid chromatography with on-line ultraviolet and mass spectrometry detection. Rapid Commun Mass Spectrom 24:1851–1868

Gouveia S, Castilho PC (2011) Characterisation of phenolic acid derivatives and flavonoids from different morphological parts of *Helichrysum obconicum* by a RP-HPLC-DAD-(-)-ESI-MS^n method. Food Chem 129:333–344

Gupta R, Sharma A, Dobhal MP, Sharma MC, Gupta RS (2011) Antidiabetic and antioxidant potential of β-sitosterol in streptozotocin-induced experimental hyperglycemia. J Diabetes 3: 29–37

Harbaum B, Hubbermann EM, Wolff C, Herges R, Zhu Z, Schwarz K (2007) Identification of flavonoids and hydroxycinnamic acids in pakchoi varieties (*Brassica campestris* L. ssp. *chinensis* var. *communis*) by HPLC-ESI-MS^n and NMR and their quantification by HPLC-DAD. J Agr Food Chem 55:8251–8260

Hawkins CL, Davies MJ (1998) Hypochlorite-induced damage to proteins: formation of nitrogen-centred radicals from lysine residues and their role in protein fragmentation. Biochem J 332:617–625

Janiak MJ, Small DM, Shipley GG (1976) Nature of the thermal pretransition of synthetic phospholipids: dimyristoyl- and dipalmitoyllecithin. Biochemistry 15:4575–4580

Katsaras J, Tristram-Nagle S, Liu Y, Headrick RL, Fontes E, Mason PC, Nagle J (2000) Clarification of the ripple phase of lecithin bilayers using fully hydrated, aligned samples. Phys Rev E 61:5668–5677

La Torre GL, Saitta M, Vilasi F, Pellicano T, Dugo G (2006) Direct determination of phenolic compounds in Sicilian wines by liquid chromatography with PDA and MS detection. Food Chem 94:640–650

Lim G, Wortis M, Mukhopadhyay R (2002) Stomatocyte–discocyte–echinocyte sequence of the human red blood cell: evidence for the bilayer-couple hypothesis from membrane mechanics. Proc Nat Acad Sci USA 99:16766–16769

Lin LZ, Sun J, Chen P, Harnly J (2011) UHPLC-PDA-ESI/HRMS/MS^n analysis of anthocyanins, flavonol glycosides, and hydroxycinnamic acid derivatives in red mustard greens (*Brassica juncea* Coss variety). J Agr Food Chem 59:12059–12072

Ling W, Jones P (1995) Dietary phytosterols: a review of metabolism, benefits and side effects. Life Sci 57:195–206

Malheiros SVP, Brito MA, Brites D, Correa MN (2000) Membrane effects of trifluoperazine, dibucaine and praziquantel on human erythrocytes. Chem-Biol Inter 126:79–95

Manrique-Moreno M, Londoño-Londoño J, Jemiola-Rzeminska M, Strzalka K, Villena F, Avello M, Suwalsky M (2014) Structural effects of the Solanum steroids solasodine, diosgenin and solanine on human erythrocytes and molecular models of eukaryotic membranes. Biochim Biophys Acta 1838:266–277

Mason PC, Nagle JF, Epand RM, Katsaras J (2001) Anomalous swelling in phospholipid bilayers is not coupled to the formation of a ripple phase. Phys Rev E 63:030902

Mesquita LG, Agero U, Mesquita ON (2006) Defocusing microscopy: an approach for red blood cell optics. Appl Phys Lett 88:133901

Montes M, Wilkomirsky T (1991) Chilean traditional medicine. University of Concepción Press, Concepcion

Mullen W, Hartley RC, Crozier A (2003) Detection and identification of 14C-labelled flavonol metabolites by high-performance liquid chromatography-radiocounting and tandem mass spectrometry. J Chromatogr A 1007:21–29

Muñoz O, Montes M, Wilkomirsky T (2004) Medicinal plants used in Chile: chemistry and pharmacology. University of Chile Press, Santiago

Obied HK, Bedgood DR Jr, Prenzler PD, Robards K (2007) Chemical screening of olive biophenol extracts by hyphenated liquid chromatography. Anal Chim Acta 603:176–189

Oszmiański J, Kolniak-Ostek J, Wojdyło A (2014) Characterization of phenolic compounds and antioxidant activity of *Solanum scabrum* and *Solanum burbankii* berries. J Agr Food Chem 62:1512–1519

Parejo I, Jauregui O, Sánchez-Rabaneda F, Viladomat F, Bastida J, Codina C (2004) Separation and characterization of phenolic compounds in fennel (*Foeniculum vulgare*) using liquid chromatography-negative electrospray ionization tandem mass spectrometry. J Agr Food Chem 52:3679–3687

Petsalo A, Jalonen J, Tolonen A (2006) Identification of flavonoids of *Rhodiola rosea* by liquid chromatography-tandem mass spectrometry. J Chromatogr A 1112:224–231

Piraud M, Vianey-Saban C, Petritis K, Elfakir C, Steghens JP, Morla A, Bouchu D (2003) ESI-MS/MS analysis of underivatised amino acids: a new tool for the diagnosis of inherited disorders of amino acid metabolism. Fragmentation study of 79 molecules of biological interest in positive and negative ionisation mode. Rapid Commun Mass Spectrom 17:1297–1311

Regueiro J, Sánchez-González C, Vallverdú-Queralt A, Simal-Gándara J, Lamuela-Raventós R, Izquierdo-Pulido M (2014) Comprehensive identification of walnut polyphenols by liquid chromatography coupled to linear ion trap-Orbitrap mass spectrometry. Food Chem 152:340–348

Schmidt S, Zietz M, Schreiner M, Rohn S, Kroh LW, Krumbein A (2010) Identification of complex, naturally occurring flavonoid glycosides in kale (*Brassica oleracea* var. *sabellica*) by high-performance liquid chromatography diode-array detection/electrospray ionization multi-stage mass spectrometry. Rapid Commun Mass Spectrom 24:2009–2022

Schrickel S, Bittner M (2001) Health in our hands. Lamas Press, Concepción

Shakya R, Navarre DA (2006) Rapid screening of ascorbic acid, glycoalkaloids, and phenolics in potato using high-performance liquid chromatography. J Agr Food Chem 54:5253–5260

Shakya R, Navarre DA (2008) LC-MS analysis of solanidane glycoalkaloid diversity among tubers of four wild potato species and three cultivars (*Solanum tuberosum*). J Agric Food Chem 56:6949–6958

Sheetz MP, Singer SJ (1974) Biological membranes as bilayer couples. A molecular mechanism of drug-erythrocyte induced interactions. Proc Nat Acad Sci USA 71:4457–4461

Shi C, Wu F, Zhu X, Xu J (2013) Incorporation of β-sitosterol into the membrane increases resistance to oxidative stress and lipid peroxidation via estrogen receptor-mediated PI3K/GSK3β signaling. Biochim Biophys Acta 1830:2538–2544

Singleton VL, Rossi JA Jr (1965) Colorimetry of total phenolics with phosphomolybdic-phosphotungstic acid reagents. Am J Enol Vitic 16:144–158

Suwalsky M (1996) Phospholipid bilayers. In: Salamone JC (ed) Polymeric materials encyclopedia. CRC, Boca Raton, pp 5073–5078

Suwalsky M, Duk L (1987) X-ray studies on phospholipid bilayers, 7. Structure determination of oriented films of L-α-dimyristoylphosphatidylethanolamine (DMPE). Makromol Chem 188:599–606

Suwalsky M, Avello M, Orellana P, Villena F (2006a) The antioxidant capacity of *Ugni imolinae* Turcz against in vitro cytotoxicity of HClO in human erythrocytes. Food ChemToxicol 45:130–145

Suwalsky M, Orellana P, Avello M, Villena F, Sotomayor CP (2006b) Human erythrocytes are affected in vitro by extracts of *Ugni molinae* leaves. Food Chem Toxicol 44:1393–1398

Suwalsky M, Vargas P, Avello M, Villena F, Sotomayor CP (2008) Human erythrocytes are affected in vitro by *Aristotelia chilensis* (Maqui) leaves. Int J Pharm 363:85–90

Suwalsky M, Oyarce K, Avello M, Villena F, Sotomayor CP (2009) Human erythrocytes and molecular models of cell membranes are affected in vitro by *Balbisia peduncularis* (Amancay) extracts. Chem-Biol Inter 179:413–418

Suwalsky M, Avello M, Obreque J, Villena F, Szymanska R, Stojakowska A, Strzalka K (2015) Protective effect of *Philesia magellanica* (Coicopihue) from Chilean patagonia against oxidative damage. J Chil Chem Soc 60:2935–2938

Tatsis EC, Boeren S, Exarchou V, Troganis AN, Vervoort J, Gerothanassis IP (2007) Identification of the major constituents of *Hypericum perforatum* by LC/SPE/NMR and/or LC/MS. Phytochem 68:383–393

Tatsumi T, Fliss H (1994) Hypochlorous acid and chloramines increase endothelial permeability: possible involvement of cellular zinc. Am J Physiol 267:H1597–H1607

Truchado P, Tourn E, Gallez LM, Moreno DA, Ferreres F, Tomás-Barberán FA (2010) Identification of botanical biomarkers in *Argentinean diplotaxis* honeys: flavonoids and glucosinolates. J Agric Food Chem 58:12678–12685

Vallverdú-Queralt A, Regueiro J, Martínez-Huélamo M, Rinaldi Alvarenga JF, Leal LN, Lamuela-Raventos RM (2014) A comprehensive study on the phenolic profile of widely used culinary herbs and spices: rosemary, thyme, oregano, cinnamon, cumin and bay. Food Chem 154:299–307

Vissers MCM, Winterbourn CC (1995) Oxidation of intracellular glutathione after exposure of human red blood cells to hypochlorousa acid. Biochem J 307:57–62

Vissers MCM, Carr AC, Chapman ALP (1998) Comparison of human red cell lysis by hypochlorous and hypobromous acids: insights into the mechanism of lysis. Biochem J 330:131–138

Yang J, Wen XD, Jia BX, Mao Q, Wang Q, Lai MX (2011) Quality evaluation of *Potentilla discolor* by high-performance liquid chromatography coupled with diode array detection and electrospray ionisation tandem mass spectrometry. Phytochem Anal 22:547–554

Ye M, Yan Y, Guo DA (2005) Characterization of phenolic compounds in the Chinese herbal drug Tu-Si-Zi by liquid chromatography coupled to electrospray ionization mass spectrometry. Rapid Commun Mass Spectrom 19:1469–1484

Zavodnik IB, Lapshina EA, Zavodnik LB, Bartosz G, Soszynski M, Bryszewska M (2001) Hypochlorous acid damages erythrocyte membrane proteins and alters lipid bilayer structure and fluidity. Free Radical Biol Med 30:363–369

Zhang Y, Liu C, Qi Y, Zhang Z (2012) Comparison of the constituents of *Apocynum venetum* and acidified *Apocynum venetum* by liquid chromatography-UV diode array detection-electrospray ionisation mass spectrometry. Med Chem Res 21:1684–1691

Zimmermann B, Soumpasis DM (1985) Effects of monovalent cations on red cell shape and size. Cell Biophys 7:115–127